Presented at the 26th European PV Solar Energy Conference and Exhibition, 5-9 September 2011, Hamburg, Germany

INTERFACE CHARACTERIZATION OF DRY-ETCHED EMITTERS

C. Clement[1], J. Seiffe[1], M. Hofmann[1], J. Rentsch[1], R. Preu[1], V. Naumann[2], M. Werner[2]
[1]Fraunhofer Institute for Solar Energy Systems, Heidenhofstr. 2, 79110 Freiburg, Germany
phone: +49 761 4588 5701, e-mail: caroline.clement@ise.fraunhofer.de
[2]Fraunhofer Center for Silicon Photovoltaics (CSP), Walter-Hülse-Str. 1, 06120 Halle, Germany

ABSTRACT: The electrical quality of a diffused phosphorous emitter can be significantly improved by etching back the defect-rich surface region (dead layer). This work focuses on the combination of a dry-etch process of the dead layer and a subsequent inline PECVD deposition of the anti-reflective coating (ARC). As we will show in the present work, the surface passivation of the ARC deposited on the plasma-etched surface is affected by a poor firing stability. At a critical temperature of about 800°C, the firing stability of the plasma-etched samples is no longer guaranteed. Therefore, the characteristics and the composition of the resulting Si/SiN_x interface play a decisive role. To investigate the reason for the firing-instability of the dry-etched samples, the interface is analyzed by transmission electron microscopy (TEM) and time-of-flight secondary ion mass spectroscopy (ToF-SIMS). The etch-back emitters show a porous interface structure with a roughness of about 10 to 20 nm and strong blistering effects in the SiN_x layer.
Keywords: interface characterisation, dry-etching, PECVD, passivation

1 INTRODUCTION

As we presented in [1], a new plasma-based solar cell concept focused on a selective etch-back emitter has been developed. The wet chemical process steps are replaced by dry plasma processes. Therefore, the process sequence takes place in an inline plasma tool. Thus less wafer handling and reduced chemical and water consumption are required, so that a fast and cost-efficient process sequence is enabled.

The application of thinner silicon wafers has become common in solar cell production, due to their inherent cost savings. This implies an increase of the ratio between the cell surface area and the cell bulk volume and hence higher recombination losses. Therefore, new emitter concepts with high surface passivation quality are required. A promising concept is represented by the etch-back emitter.

By etching back the defect-rich surface region (dead layer) and subsequently depositing the ARC layer on top of it, the energy conversion efficiency increases [2]. Dastgheib-Shirazi et al [2] execute the etch-back process in a wet-chemical HF/HNO_3-solution.

In the work presented here, the etch-back procedure is performed by a dry-etching process in a plasma inline tool (cf. [1]). The subsequent PECVD deposition of the silicon nitride (ARC) layer proceeds inline without leaving the vacuum environment.

In an earlier work [1], we showed that a homogenous removal of the dead layer improves the electrical quality of an emitter. By etching-back an initial 60 Ω/sq emitter to $R_{sh} = 141$ Ω/sq, an emitter saturation current of $J_{oe} = 57$ fA/cm^2 was achieved (using shiny-etched FZ wafers).

To continuously improve the etch-back emitter, more knowledge about the characteristics of the interface between the etched silicon surface and the deposited ARC layer (Si/SiN_x interface) is necessary. This work focuses on analyzing the interface by transmission electron microscopy (TEM) and time-of-flight secondary ion mass spectroscopy (ToF-SIMS) measurements. Furthermore, the firing stability of the dry-etched emitter will be evaluated.

2 EXPERIMENTAL

The plasma etching and the subsequent ARC deposition took place in the same vacuum chamber of a semi-inline plasma tool (SiNA; Roth&Rau), hence the samples do not leave the vacuum between steps. The plasma is generated by a microwave linear antenna at a frequency of 2.45 GHz. The carrier, with a width of 90 cm, proceeds below the plasma sources, so that the samples are etched and deposited from above. In Figure 1, a schematic diagram illustrates the construction of the used plasma tool.

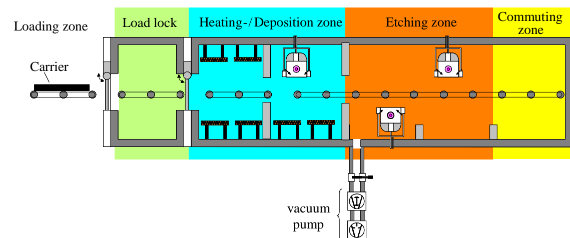

Figure 1: Semi-inline plasma tool (SiNA , Roth&Rau) used in this work [3].

Within this work, p-type (boron-doped) float-zone silicon wafers ($\rho = 1$ Ωcm) with a shiny-etched surface are used. After a thermal diffusion process, all wafers exhibited a 60 Ω/sq emitter. Next, a wet-chemical removal of the phosphosilicate glass (PSG) was performed. After these preparation steps, the samples are treated with the plasma etch and deposition process in the plasma tool. That means that the wafers are etched on both sides with sulphur hexafluoride (SF_6) to remove the defect-rich dead layer and subsequently deposited with a standard amorphous hydrogenated silicon nitride (a-SiN_x:H, or in short: SiN_x) as ARC layer. The application of this process sequence is varied as follows

- At the standard process, the samples are SF_6 plasma etched for about 3.5 s at a pressure p_{st}. The samples are then subsequently coated with a SiN_x layer.

- SF_6 plasma etched samples processed at a lower pressure p_{low} are used for comparison. Apart from that, they are treated like in the standard process.

- To improve the process sequence, an additional ammonia (NH_3) plasma cleaning for about 8.8 s is partially appended between the SF_6 plasma etching and the SiN_x deposition. This additional cleaning process removes potentially remanent etch residues from the silicon surface before the ARC layer is deposited on top of it. Thus, the blistering effects are reduced and the passivation quality as well as the firing stability is further improved [4, 5].

- Reference samples are deposited directly after the PSG removal without any plasma etching or plasma cleaning step in between.

All these process sequences take place in one and the same vacuum chamber, so that all steps proceed at a temperature of 350°C.

All wafers are etched and deposited on both sides. Thus, only symmetrical samples are produced.

The resultant effective charge carrier lifetime is examined by using a quasi-steady-state photoconductance (QSSPC) measurement tool (WCT-100, Sinton). The lifetime measurement is done before and after the fast-firing step to analyze the firing stability of the samples. The firing temperature is varied between 650 °C and 880 °C.

In order to investigate the characteristics and the morphology of the interface between the etched silicon surface and the deposited ARC layer, TEM and ToF-SIMS measurements have been performed.

In Figure 2, an overview of all presented process sequences is shown.

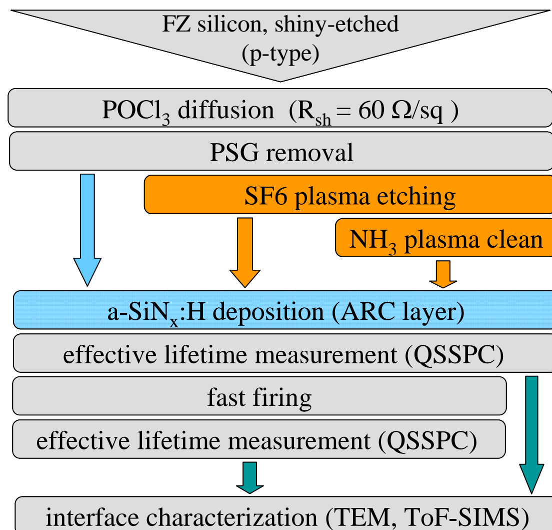

Figure 2: Process sequences proceeding in this work.

3 RESULTS AND DISCUSSION

3.1 Results of the effective lifetime measurements (QSSPC)

To check the firing stability of the dry-etched samples, quasi-steady-state photoconductance (QSSPC) measurements of the effective carrier lifetime τ_{eff} in dependence of the firing temperature have been performed (one sample per measuring point, except for "before firing"). The results are summarised in Figure 3. Additionally, the emitter saturation current J_{0e} is determined using [6]

$$J_{0e} = \frac{q n_i^2 W}{2(N_{dop} + \Delta n)} \left\{ \frac{1}{\frac{1}{\tau_{eff}} - \frac{1}{\tau_{bulk}}} - \frac{1}{D_{min}} \left(\frac{W}{\pi} \right)^2 \right\}^{-1} \qquad (1)$$

with the elementary charge q, the intrinsic carrier density $n_i = 9.143 \times 10^9$ cm^{-3} [7], the wafer thickness W, the doping concentration N_{dop}, the minority excess charge carrier density Δn and the minority diffusion constant D_{min}. For the calculation of the bulk lifetime τ_{bulk}, the Auger-recombination model of Kerr and Cuevas [8] was used.

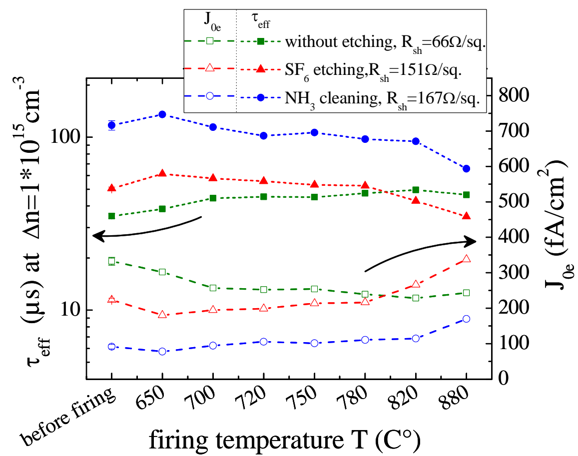

Figure 3: Quasi-steady-state photoconductance (QSSPC) measurements of the effective carrier lifetime and emitter saturation currents as calculated from the lifetime results, both in dependence of the firing temperature.

Figure 3 shows that for the etch-back emitter (△,○) the passivation quality improves up to a temperature of 780°C. Two different dry-etching processes are plotted: the ARC-SiN_x layer is deposited either directly after the SF_6 plasma etch process (△) or after an additional NH_3 plasma cleaning step (○). The latter clearly represents the best passivation qualities with effective carrier lifetimes τ_{eff} around 100 µs. For example, at a temperature of 780 °C an effective carrier lifetime τ_{eff} of 97 µs is reached, which corresponds to an emitter saturation current J_{oe} of 111 fA/cm^2. For comparison, the passivation quality of the only SF_6 plasma etched sample results in J_{oe} = 216 fA/cm^2 (at 780 °C).

With increasing temperature, especially above 800°C, the effective carrier lifetime decreases for the dry-etched samples (△,○), whereas the purely wet-chemically treated samples (□) indicate a good firing stability.

The reasons for this firing instability will be attempted to be found by means of interface analysis.

3.2 Results of the interface characterization

The transmission electron microscopy (TEM) images illustrate the interface formation. In Figure 4 a purely wet-chemically treated (left) and a dry-etched (right) sample are shown for comparison. The latter one was etched with the standard SF_6 plasma process without any additional NH_3 plasma cleaning in between.

The unetched sample presents a clear and well-defined Si/SiN_x interface. In addition, the SiN_x layer grew up homogeneously. In contrast, the plasma-etched sample shows a porous interface structure with a roughness of about 10 to 20 nm. Moreover, gas cavities perforate the SiN_x layer (blistering effect), leading to an inhomogeneous layer growth. On the rough interface, hydrogen accumulation is becoming more probable, so that the development of hydrogen clusters is intensified. Hence, the blistering effect is increased.

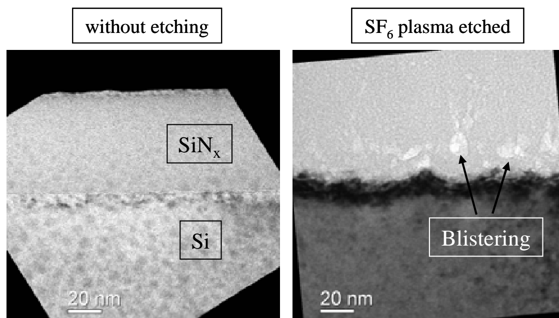

Figure 4: TEM images of the unetched reference sample (left) and the SF_6 plasma etched sample (right).

In compliance with the work of Hauser [4, 5] and de Wolf [4, 5], the additional NH_3 plasma cleaning prior to the SiN_x deposition gives rise to advanced passivation qualities (cf. section 3.1). In the previous works, this was attributed to a reduced blistering effect. This finding cannot be confirmed here. Considering the TEM images in Figure 5, the standard SF_6 plasma etched sample (left) and the sample with an additional NH_3 plasma cleaning (right), both show a rough interface structure and a blistering effect to the same extent. Therefore, the NH_3 plasma cleaning does not decrease the blistering in the SiN_x layer.

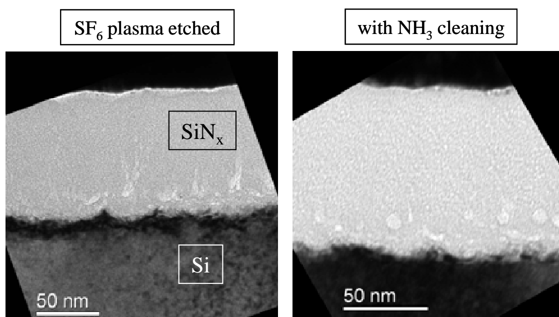

Figure 5 : TEM images of the SF_6 plasma etched sample (left) and the sample with an additional NH_3 plasma cleaning (right).

In order to investigate etch residues on the Si/SiN_x interface, the samples are analyzed by time-of-flight secondary ion mass spectroscopy (ToF-SIMS). By means of the ToF-SIMS analysis, element-specific depth profiles were obtained. By using these profiles, the Si/SiN_x interface was estimated using the silicon signal.

The ToF-SIMS measurements in Figure 6 show that the wet-chemically treated interface (top) is narrower than the standard SF_6 plasma etched one (bottom). This is in support of the increased roughness in the dry-etched samples exhibited by the TEM measurements (identical samples as used for Figure 4). Moreover, the surface roughness is increasing through sedimentation of etch residues. Both effects lead to an amplified blistering effect and hence to firing instabilities.

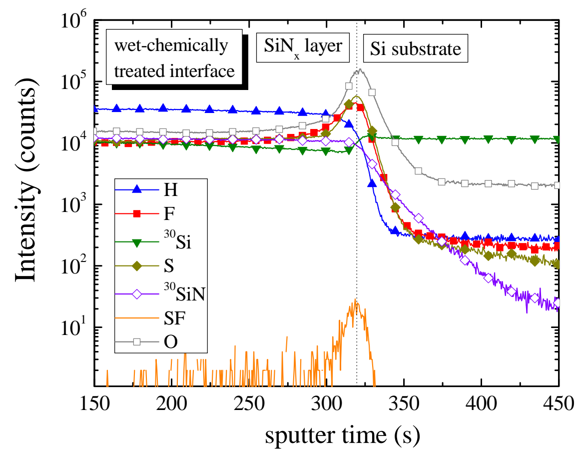

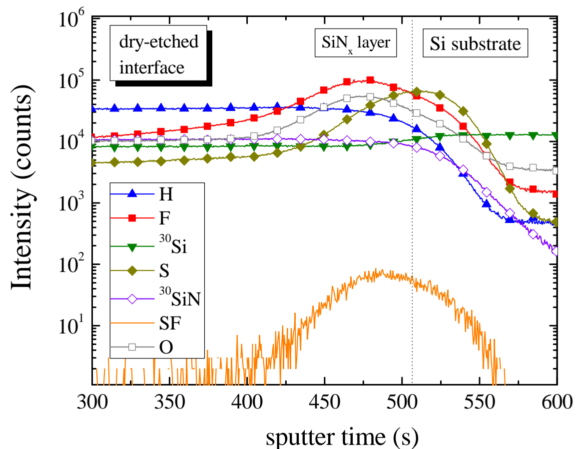

Figure 6: ToF-SIMS depth profiles of the wet-chemically treated sample (top) and the dry-etched sample (bottom).

Figure 7 and Figure 8 demonstrate that, especially for the SF_6 plasma etched samples (p_{st} and p_{low}), the oxygen (O), the sulfur fluoride (SF) and the fluorine (F) peak are shifted into the SiN_x layer (to a lesser depth). It seems likely that due to oxygen contaminations in the process chamber and fluorine residues, discontiguous $Si_xO_yF_z$ islands deposit on the silicon surface, which might harm the etching process in some places. Thus, a roughness structure on the Si/SiN_x interface occurs. An additional NH_3 cleaning could likely reduce this effect.

In the texture process described in [9], such a $Si_xO_yF_z$ adsorbate film is used for masking. According to this fact, the dead layer etching process could create a texture on a nanometer scale.

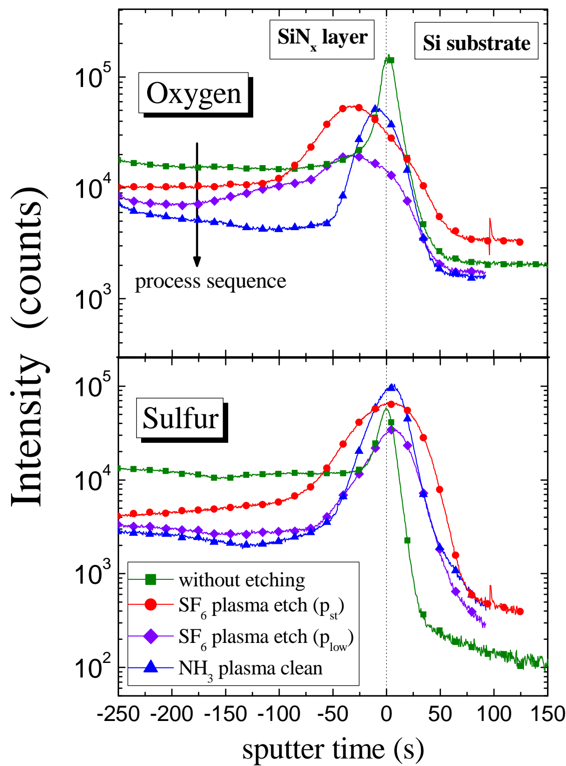

Figure 7: ToF-SIMS depth-profiles of oxygen (top) and sulfur (bottom). The oxygen and sulfur contaminations on the Si/SiN_x interface of the differently processed samples can therefore be compared.

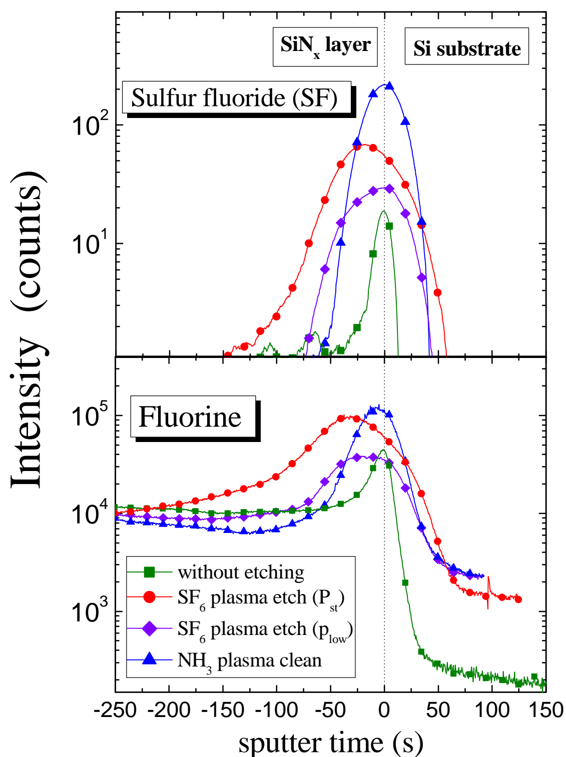

Figure 8: ToF-SIMS depth profiles of sulfur fluoride (top) and fluorine (bottom). This allows comparison of the etch residues on the Si/SiN_x interface between the different processes.

Furthermore, a correlation between the temporal process sequence and the oxygen, as well as the sulfur content within the SiN_x layer was investigated (cf. Figure 7). As shown in Figure 7, the SiN_x layer contains fewer contaminations like oxygen or sulfur with increasing operating time of the inline plasma tool.

The dry etched samples present a firing instability at a critical temperature of about 800 °C, as shown by effective lifetime measurements in section 3.1. By means of ToF-SIMS measurements, it was investigated whether a difference in the depth profiles of firing-instable and firing-stable samples is identifiable. Therefore, samples with an additional NH_3 cleaning were analyzed before and after the high-temperature process. The resulting depth profiles are represented in Figure 9.

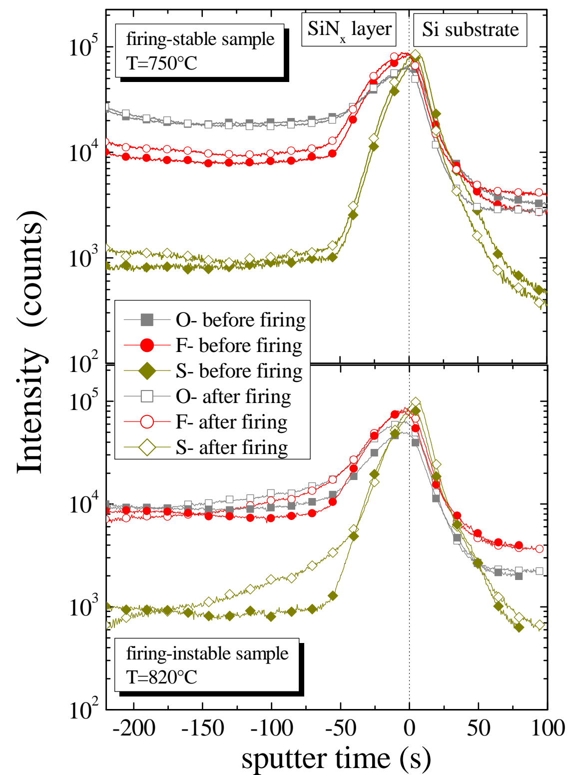

Figure 9: Comparison of ToF-SIMS measurements before and after the firing step.

The depth profiles of the firing-stable sample show no obvious difference between the profiles before and after the firing step, whereas the profile of the firing-instable sample exhibits that sulfur, fluorine and oxygen are shifted into the SiN_x layer (to a lesser depth) after the high-temperature treatment. This indicates that these elements diffuse into the ARC layer during the high-temperature process. This is one reason for the assumption that sulfur oxifluoride ($S_xO_yF_z$) compositions occur on the Si/SiN_x interface, which accumulates on the rough surface. At high-temperature processes, $S_xO_yF_z$ blisters are created, which then diffuse into the SiN_x layer. It could be possible that, in addition to hydrogen bubbles, also $S_xO_yF_z$ blisters lead to the appearance of the blistering effect.

4 SUMMARY AND CONCLUSION

By means of temperature variation at the firing step, it is shown that the dry-etched emitter improves the passivation quality up to a temperature of about 800 °C. At 800°C a critical temperature is reached, above which firing stability is no longer guaranteed.

Sensitive tools for the interface characterization between the ARC and the silicon have been used to investigate the reason for the poor firing stability.

The TEM and ToF-SIMS measurements indicate that the dry-etched samples do have a rough interface morphology, whereas the only wet-chemically treated reference samples show a well-defined and clear interface structure. Additionally, both at the SF_6 plasma etched sample and at the sample with additional NH_3 cleaning, blistering appears in the SiN_x layer. The roughness, as well as the blistering effect, does lead to firing instabilities.

The TEM images demonstrate that the NH_3 plasma cleaning does not harm the blistering effect. Perhaps the reason for the improved passivation quality is given by the additionally provided amount of hydrogen in the ammonia plasma. This amount of hydrogen, along with the hydrogen of the ARC layer, contributes to the surface passivation.

Moreover, the results of the ToF-SIMS measurements suggest that the blistering is intensified by $S_xO_yF_z$ gas cavities. Furthermore, the interface roughness can probably be traced back to a deposited $Si_xO_yF_z$ adsorbate film which harms the etching process in places, resulting in the formation of bumps.

4 ACKNOWLEDGEMENTS

The authors would like to thank Heike Furtwängler and Rainer Neubauer for the wet-chemical cleaning, Andreas Müller for the $POCL_3$ diffusion and Pasquale Malm for the firing step.

Furthermore the authors gratefully acknowledge the help of all co-workers at the Fraunhofer Center for Silicon Photovoltaics in Halle for the TEM and ToF-SIMS measurements.

This work was partly funded by the German Federal Ministry of Education and Research (BMBF) under contract no. 13N11838

5 REFERENCES

[1] J. Seiffe, et al., Proceedings of the 25th European Photovoltaic Solar Energy Conference Valencia, Spain (2010).
[2] A. Dastgheib-Shirazi, et al., Proceedings of the 23rd European Photovoltaic Solar Energy Conference, Valencia, Spain (2008) 1197.
[3] M. Hofmann. in Fachbereich Physik, pp. 273, Universität Konstanz, Freiburg im Breisgau 2008.
[4] A. Hauser, et al., Solar Energy Materials and Solar Cells 75 (2003) 357.
[5] S. de Wolf, et al., Proceedings of the 20th European Photovoltaic Solar Energy Conference, Barcelona, Spain (2005) 729.
[6] A. Cuevas, et al., Solar Energy 76 (2004) 255.
[7] A.B. Sproul, et al., Journal of Applied Physics 73 (1993) 1214.
[8] M.J. Kerr, et al., Journal of Applied Physics 91 (2002) 2473.
[9] H. Jansen, et al., Black Silicon Method, (1995).